

Characterization of Regions of Change of Simulated Droughts and Floods of Water Bodies

S. Dinesh

Science and Technology Research Institute for Defence (STRIDE), Ministry of Defence, Malaysia.

Abstract: Change detection is the process of identifying differences in the state of an object or phenomenon by observing it at different times. Change detection is an important process in monitoring and managing natural resources and urban development because it provides quantitative analysis of the spatial distribution of the population of interest. In this paper, the characterization of regions of change of simulated droughts and floods of water bodies is performed. Power law relationships are observed between the areas of regions of change of simulated droughts/floods and the droughting/flooding levels. These power law relationships arise as a consequence of the fractal properties of the regions of change of simulated droughts and floods of water bodies. The scaling exponent of these power laws, which is named as a fractal dimension, indicates the rate of variation of areas of regions of change of water bodies over varying levels of droughting/flooding. The identified regions of change are employed to compute two fundamental complexity measures of the simulated droughts and floods of water bodies; average area and average uncertainty. It is observed that simulated droughts have higher values of average size and average uncertainty as compared to simulated floods, as simulated droughts diverge from the self organized criticality, while simulated floods converge towards the self organized criticality.

Key words: water bodies; simulated droughts and floods; regions of change; fractal dimension; complexity measures; self organized criticality.

INTRODUCTION

Change detection is the process of identifying differences in the state of an object or phenomenon by observing it at different times ^[1-4]. Change detection is an important process in monitoring and managing natural resources and urban development because it provides quantitative analysis of the spatial distribution of the population of interest. Macleod and Congation ^[5] listed four aspects of change detection which are important when monitoring natural resources; detecting the changes that have occurred, identifying the nature of the change, measuring the area extent of the change, and assessing the spatial pattern of the change.

The basis of using remote sensing data for change detection is that changes in land cover result in changes in radiance values which can be remotely sensed. Techniques to perform change detection with satellite imagery have become numerous as a result of increasing versatility in manipulating digital data and increasing computer power. A wide variety of digital change detection techniques have been developed over the last two decades; a summary is provide in Singh ^[1], Coppin and Bauer ^[6], Lu *et al.* ^[2], Radke *et al.* ^[2], and Zubair ^[4].

In this paper, the characterization of regions of change of simulated droughts and floods of water bodies is performed. It is demonstrated, via power law relationships, the fractal properties of regions of change of simulated droughts and floods of water bodies. The regions of change are employed to compute two fundamental complexity measures of simulated droughts and floods of water bodies, average area and average uncertainty, which are used to identify the level of convergence/divergence of simulated droughts/floods of water bodies from the self organized criticality.

MATERIAL AND METHODS

2.1 The Data Set: Gothavary River, which lies in central India, originates near Triambak in the Nasik district of Maharashtra, and flows through the states of Madhya Pradesh, Karnataka, Orissa and Andhra Pradesh. Although its point of origin is just 80 km away from the Arabian Sea, it journeys 1,465 km to empty into the Bay of Bengal. Some of its tributaries include Indravati, Manjira, Bindusara and Sarbari. Some important urban centers on its banks include Nasik, Aurangabad, Nagpur, Nizamabad, Rajahmundry, and Balaghat. The Gothavary River is often referred to

Corresponding Author: S. Dinesh, Science and Technology Research Institute for Defence, D/A KD Malaya, Pangkalan TLDM, 32100 Lumut, Perak.
Tel: 6013-5941144
E-mail: dinsat60@hotmail.com

as the Vriddh (Old) Ganga or the Dakshin (South) Ganga. The Gothavary River catchment has an area of 312, 870 km² and receives more than 85% of its annual rainfall during the monsoon season (June-September). Hence, the water resources in this river are largely due to monsoon rainfall, and largely affected by monsoon extremities, resulting in floods during some years and droughts during others.

Figure 1(a) shows a number of water bodies of varying shape and sizes situated in a portion of the floodplain region of Gothavary River. The water bodies were traced from Indian Remote Sensing Satellites (IRS) 1D remotely sensed data. The IRS-1D was launched on 28 September 1997 by the Indian Space Research Organization (ISRO) operated Polar Satellite Launch Vehicle (PSLV). The data was captured using the multispectral Linear Imaging Self-Scanning Sensor 3 (LISS-3) with spatial resolution 23.7 m and band range of 520-590 nm. Due to the impracticalities of dealing with incomplete water bodies, these incomplete water bodies are removed, and only the complete water bodies are considered (Figure 1(b)). A total of 67 distinct individual water bodies (Figure 1(c)) are identified using connected component labeling [7].

2.2 Generation of Simulated Droughts and Floods of Water Bodies: Mathematical morphology is a branch of image processing that deals with the extraction of image components that are useful for representational and descriptive purposes. Mathematical morphology has a well developed mathematical structure that is based on set theoretic concepts. The effects of the basic morphological operations can be given simple and intuitive interpretations using geometric terms of shape, size and location. The fundamental morphological operators are discussed in Matheron [8], Serra [9] and Soille [10]. Morphological operators generally require two inputs; the input image *A*, which can be in binary or grayscale form, and the kernel *B*, which is used to determine the precise effect of the operator.

Dilation sets the pixel values within the kernel to the maximum value of the pixel neighbourhood. Binary dilation fills the small holes inside particles and gulfs on the boundary of objects, enlarges the size of the particles and may connect neighbouring particles [11]. The dilation operation is expressed as:

$$A \oplus B = \{a+b: acA, bcB\} \tag{1}$$

Erosion sets the pixels values within the kernel to the minimum value of the kernel. Binary erosion removes isolated points and small particles, shrinks other particles, discards peaks on the boundaries of objects, and disconnects some particles [11]. Erosion is the dual operator of dilation:

$$A \ominus B = (A^c \oplus B)^c \tag{2}$$

where *A*^c denotes the complement of *A*, and *B* is symmetric with respect to reflection about the origin.

Drought and flood simulation is implemented by performing erosion and dilation, respectively, on water bodies using square kernels of increasing size [12-15]. Erosion reduces the area of water bodies, mimicking droughting, while dilation increases the area of water bodies, mimicking flooding. The level of droughting/flooding is indicated by the kernel size.

Simulated droughts (Figure 2) and floods (Figure 3) of the water bodies for levels of 1 to 15 are computed. The areas of the generated simulated droughts and floods are shown in Table 1.

Table 1: Areas of the generated simulated droughts and floods of the water bodies.

Level	Area (pixels)	
	Drought	Flood
1	137837	137837
2	123336	152789
3	109565	167979
4	96328	183647
5	83764	199532
6	71844	215862
7	60839	232283
8	51141	249127
9	42863	265919
10	35980	283048
11	30230	300047
12	25380	317358
13	21220	334503
14	17737	351937
15	14794	369093

2.3 Detection of Regions of Change: The regions of change of the simulated droughts (Figure 4) and floods (Figure 5) are computed. The area of the regions of change *S(r)* for each droughting/flooding level *r* is shown in Table 2.

Table 2: Areas of change of the simulated droughts and floods of the water bodies.

Level	Area of change (pixels)	
	Drought	Flood
2	3732	3666
3	3548	3778
4	3374	3896
5	3197	4013
6	2893	4123
7	2649	4200
8	2380	4262
9	1956	4322
10	1748	4346
11	1556	4376
12	1151	4392
13	974	4421
14	836	4446
15	742	4449

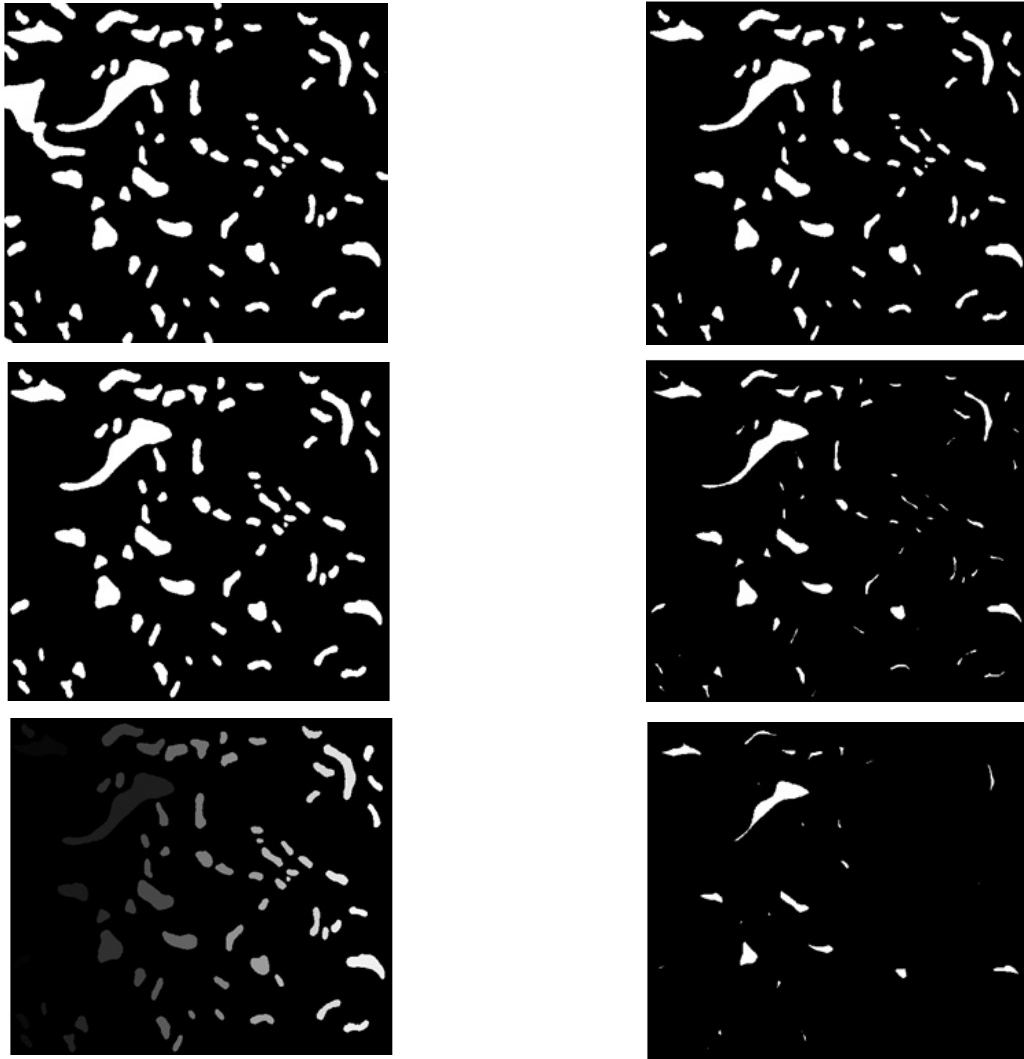


Fig. 1: Water bodies of varying shapes and sizes situated in a portion of the flood plain region of Gothavary River. (a) The original water bodies traced from IRS 1D remotely sensed data. (b) The water bodies after removal of incomplete water bodies. (c) Identification of the individual water bodies using connected component labeling. The water body count number is determined by the grey level; the brighter the grey level, the larger the water body count number.

RESULTS AND DISCUSSION

Log-log plots of the area of the regions of change $S(r)$ against the droughting/flooding level r are drawn for the simulated droughts (Figure 6(a)) and floods (Figure 6(b)). Power law relationships are observed in both plots. These power laws take the following form:

Fig. 2: The generated simulated droughts of the water bodies at droughting levels of: (a) 3 (b) 7 (c) 11 (d) 15.

$$S(r) = c * r^D \tag{3}$$

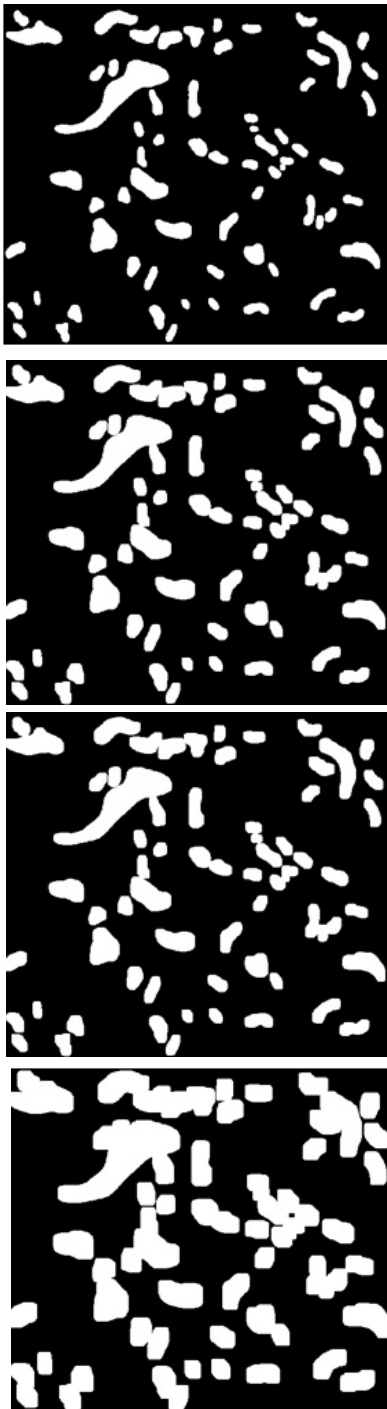


Fig. 3: The generated simulated floods of the water bodies at flooding levels of: (a) 3 (b) 7 (c) 11 (d) 15.

These power law relationships arise as a consequence of the fractal properties of the regions of change of droughts and floods of water bodies. The term 'fractal' implies that an object or pattern has self-

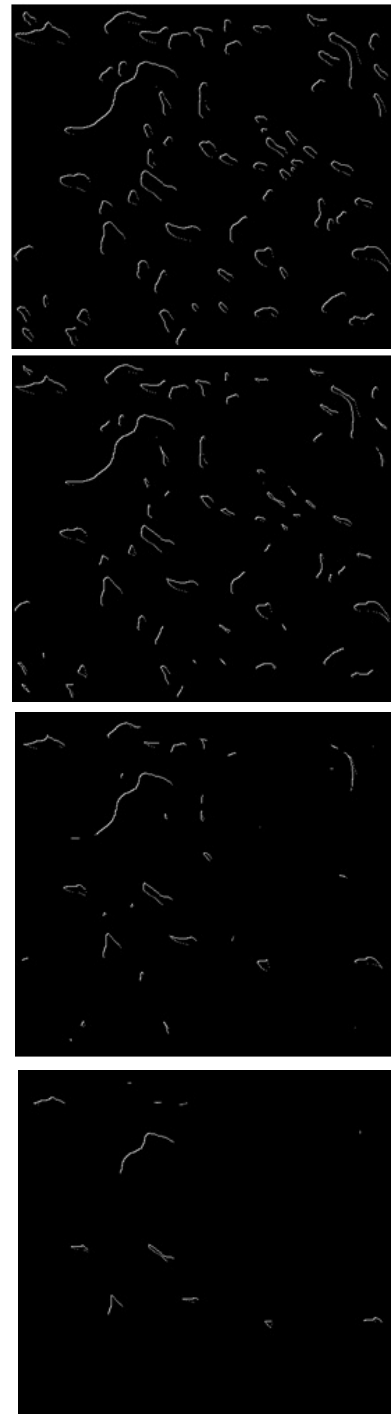


Fig. 4: Areas of change of the corresponding simulated droughts in Figure 2.

similar or self-affine properties. Self-similar means that parts of an object are identical to the whole, and self-affine means that parts of an object resemble systematically squashed or stretched versions of the wholes. Ideal fractals display similarity across an

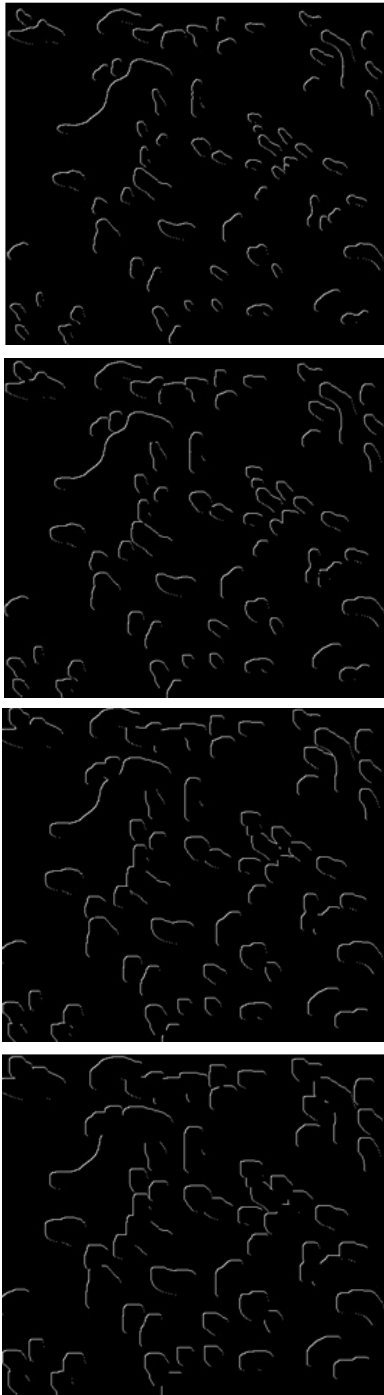


Fig. 5: Areas of change of the corresponding simulated floods in Figure 3.

infinite range of scales, which is rarely seen in nature. Consequently, the ranges of fractality can be used to decipher characteristic scales and thresholds at which physical processes operate. Fractal geometry was introduced and popularized by Mandelbrot [16-18] to

describe highly complex forms that are characteristic of natural phenomena such as coastlines and landscapes. In Equation 3, c is a constant of proportionality, while D is the fractal dimension of the regions of change of the simulated droughts/floods of water bodies, which indicates the rate of variation of areas of regions of change of simulated droughts/floods water bodies over varying levels of droughting/flooding. D has a positive value for increasing areas of regions of change, and a negative value for decreasing areas of regions of change.

The identified regions of change can be employed to compute two fundamental complexity measures of the simulated droughts and floods of water bodies; average area and average uncertainty [19]. The normalized probability function of the regions of change $s(r)$ at droughting/flooding level r is computed as follows:

$$s(r) = S(r)/S_0(r) \quad (4)$$

where $S_0(r)$ is the area of water bodies at r .

A plot of the normalized probability functions against the droughting/flooding levels is drawn (Figure 7). It is observed that $s(r)$ increases as the droughting level is increased, and decreases as the flooding level is increased.

Self organized criticality is exhibited by dynamic systems which reach a critical state of equilibrium by their intrinsic dynamics, independently of the value of any control parameter [20-24]. During flooding processes, randomly situated water bodies of varying sizes and shapes tend to self organize. At high degrees of flooding intensity, water bodies contact together to form influence zones, which indicate the self organized criticality of the flooding of water bodies [25-27]. Droughting causes the water bodies to diverge from the self organized criticality, and hence, $s(r)$ increases. Flooding causes the water bodies to converge towards the self organized criticality, and hence $s(r)$ decreases.

The computed values of $s(r)$ are used to compute two important complexity measures:

Average size AS : This indicates the average size of regions of change of simulated droughts/floods of water bodies.

Average Uncertainty H : Quantifies the shape-size complexity of the regions of change simulated droughts/floods of water bodies.

AS and H are computed using the following equations, which are due to Maragos [19]:

$$AS = \sum_{r=1}^{20} r s(r) \quad (4)$$

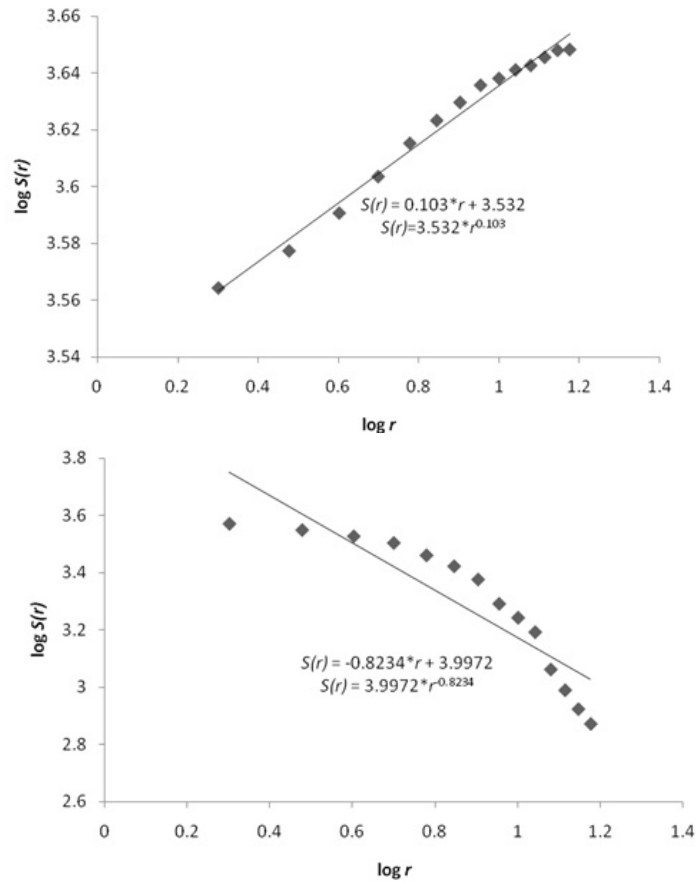


Fig. 6: Log-log plots of the area of change $S(r)$ against the droughting/flooding level r . (a) Simulated droughts. (b) Simulated floods.

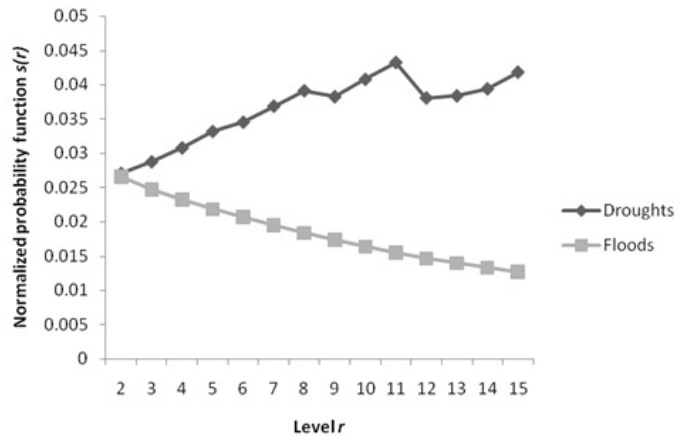


Fig. 7: Plot of the normalized probability function $s(r)$ against the droughting/flooding level r .

$$H = \sum_{r=1}^{20} s(r) \log s(r) \quad (5)$$

AS and H are computed to be 4.57 and 0.73, respectively, for simulated droughts, and 1.96 and 0.45, respectively, for simulated floods. Simulated droughts have higher values of AS and H as compared to

simulated floods, as simulated droughts diverge from the self organized criticality, while simulated floods converge towards the self organized criticality.

Conclusion: In this paper, the characterization of regions of change of simulated droughts and floods of water bodies was performed. Power law relationships

were observed between the areas of regions of change of simulated droughts/floods and the droughting/flooding levels. These power law relationships arise as a consequence of the fractal properties of the regions of change of simulated droughts and floods of water bodies. The scaling exponent of these power laws, which was named as a fractal dimension, indicates the rate of variation of areas of regions of change of water bodies over varying levels of droughting/flooding. The identified regions of change were employed to compute two fundamental complexity measures of the simulated droughts and floods of water bodies; average area and average uncertainty. It was observed that simulated droughts have higher values of average size and average uncertainty as compared to simulated floods, as simulated droughts diverge from the self organized criticality, while simulated floods converge towards the self organized criticality.

It is important to note that in this paper, droughting and flooding simulations are performed on the assumption that floodplain regions, which have a maximum gradient of less than 2° , approximate isotropic surfaces. However, this assumption does not hold for other areas with gradients higher than 2° . In these cases, droughting and flooding simulation will need to take into consideration the gradient computed from the corresponding elevation maps. Furthermore, while the study of the Gothavary River floodplain does provide interesting results in regards to a region that undergoes significant spatio-temporal changes due to droughts and floods, the conclusions drawn from the study of this region does not necessarily apply to all regions. At present, work is being done to study the regions of change of simulated droughts and floods of water bodies of regions of varying geomorphological topographies in order to study the generality of the findings of this paper.

REFERENCES

1. Singh, A., 1989. Digital change detection techniques using remotely sensed data. *International J. Remote Sensing*, 10(6): 989- 1003.
2. Lu, D., P. Mausel, E. Brondiacutezio and E. Moran, 2004. Change detection techniques. *International J. Remote Sensing*, 25(12): 2365-2401.
3. Radke, R.J., S. Andra, O. Al-Kofahi and B. Roysam, 2005. Image change detection algorithms: A systematic survey. *IEEE Transactions on Image Processing*, 14(3): 294-307.
4. Zubair, A.O, 2006. Change Detection in Land Use and Land Cover Using Remote Sensing Data and GIS: A Case Study of Ilorin and Its Environs in Kwara State. Masters Thesis, University Of Ibadan, Nigeria.
5. Macleod, R.D. and R.G. Congalton, 1998. A quantitative comparison of change detection algorithms for monitoring eelgrass from remotely sensed data. *Photogrammetric Engineering & Remote Sensing*, 64(3): 207-216.
6. Coppin, P. and M. Bauer, 1996. Digital change detection in forest ecosystems with remote sensing imagery. *Remote Sensing Reviews*, 13: 207-234.
7. Pitas, I., 1993. *Digital Image Processing Algorithms*. Prentice Hall, London.
8. Matheron, G., 1975. *Random Sets and Integral Geometry*, Wiley, New York.
9. Serra, J., 1982. *Image Analysis and Mathematical Morphology*. Academic Press, London.
10. Soille, P., 2003. *Morphological Image Analysis: Principles and Applications*. Springer Verlag, Berlin.
11. Duchene, P. and D. Lewis, 1996. *Visilog 5 Documentation*. Noesis Vision, Quebec.
12. Dinesh, S., 2007. Convex characterization of simulated droughts and floods of water bodies. *Journal Applied Sciences*, 7(11): 1516-1521.
13. Dinesh, S., 2007. Characterization of convexity of simulated droughts and floods of water bodies. *World Engineering Congress 2007 (WEC 2007)*, 5th-9th August 2007, Penang.
14. Dinesh, S., 2007. Analysis of influence zones of simulated droughts and floods of water bodies, *Joint International Symposium & Exhibition on Geoinformation and GPS/GNSS 2007 (ISG & GPS/GNSS 2007)*, 5th to 7th November 2007, PERSADA Johor International Convention Centre, Johor Bahru.
15. Dinesh, S., 2008. Characterization of influence zones of simulated droughts and floods of water bodies in a floodplain. *Computers & Geosciences*, 34(12): 1791-1797.
16. Mandelbrot, B.B., 1967. How long is the coast of Britain? Statistical self-similarity and fractional dimension. *Science*, 156: 636-638.
17. Mandelbrot, B.B., 1977. *Fractals: Form, Chance and Dimension*. Freeman, San Francisco, California.
18. Mandelbrot, B.B., 1982. *The Fractal Geometry of Nature*. Freeman, San Francisco, California.
19. Maragos, P., 1989. Pattern spectrum and multiscale shape representation. *IEEE Transactions on Pattern Analysis and Machine Intelligence*, 11(7): 701-716.
20. Bak, P., C. Tang and K. Wiesenfeld, 1987. Self-organized criticality: An explanation of $1/f$ noise. *Physical Review Letters*, 59: 381-384.
21. Bak, P., C. Tang and K. Wiesenfeld, 1988. Self-organized criticality, *Physical Review A*, 38: 364-374.
22. Bak, P., 1996. *How Nature Works: The Science of Self-Organized Criticality*, Copernicus New York.

23. Jensen, H.J., 1998. *Self-Organized Criticality*. Cambridge University Press, Cambridge.
24. Garlaschelli, D., A. Capocci and G. Caldarelli, 2007. Self-organized network evolution coupled to extremal dynamics, *Nature Physics*, 3: 813 - 817.
25. Sagar, B.S.D., 2001. Generation of self organized critical connectivity network map (SOCCNM) of randomly situated surface water bodies. *Discrete Dynamics in Nature and Society*, 6(3): 225-228.
26. Sagar, B.S.D., 2005. Discrete simulations of spatio-temporal dynamics of small water bodies under varied streamflow discharges. *Nonlinear Processes in Geophysics*, 12: 31-40.
27. Sagar, B.S.D., 2007. Universal scaling laws in surface water bodies and their zones of influence, *Water Resources Research*, 43(2): W02416, doi:W06502,10.1029/2006WR005075.